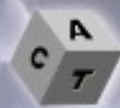


# Journal of Advanced Concrete Technology

## Materials, Structures and Environment



### Double-Counting Problem of FEA with Simultaneous Use of Bond Link Elements and Tension-Stiffening Model

Yuichi Sato, Toshiyuki Kanakubo, Hiroshi Shima

*Journal of Advanced Concrete Technology*, volume 11 (2013), pp. 206-214

#### Related Papers [Click to Download full PDF!](#)

##### **R/C Frame Structures with Beams Wrapped by Aramid Fiber Reinforced Polymer Sheets**

Wael A. Zatar, Hiroshi Mutsuyoshi

*Journal of Advanced Concrete Technology*, volume 2 (2004), pp. 49-63

##### **Punching Shear Failure Mechanism of Open Sandwich Slab and its Parameters' Effects**

Ahmed Farghaly, Hitoshi Furuuchi, Tamon Ueda

*Journal of Advanced Concrete Technology*, volume 3 (2005), pp. 283-296

##### **Nonlinear Finite Element Analysis on Shear Failure of Structural Elements Using High Performance Fiber Reinforced Cement Composite**

Haruhiko Suwada, Hiroshi Fukuyama

*Journal of Advanced Concrete Technology*, volume 4 (2006), pp. 45-57

[Click to Submit your Papers](#)

Japan Concrete Institute <http://www.j-act.org>



## Scientific paper

# Double-Counting Problem of FEA with Simultaneous Use of Bond Link Elements and Tension-Stiffening Model

Yuichi Sato<sup>1</sup>, Toshiyuki Kanakubo<sup>2</sup> and Hiroshi Shima<sup>3</sup>

Received 23 July 2012, accepted 17 August 2013

doi:10.3151/jact.11.206

## Abstract

This paper presents an analytical investigation of the double-counting problem in finite element analyses in which bond link elements, discrete reinforcement elements, and tension-stiffening models are used simultaneously. Engineers and researchers often use the bond link elements in the FEA to express bond slip between reinforcing bar and concrete. On the other hand, in case of smeared crack modeling, bond behavior is indirectly expressed by a tension-stiffening model of concrete. If the bond link elements and tension-stiffening models are used simultaneously, there is some concern that the effect of the bond is double counted. Hence, example uniaxial tension specimens are analyzed by three different analysis methods to investigate the double-counting effect. (1) Smeared crack analyses present no double-counting effect while (2) discrete crack analyses cause the double counting of tensile concrete stresses and result in over cracking. (3) Discrete crack analyses with delayed cracking also cause double counting although over cracking does not occur but the tension-stiffening relationships are overestimated.

## 1. Introduction

This paper deals with the double-counting problem caused by simultaneous use of discrete reinforcement elements, bond link elements, and tension-stiffening models.

Since Ngo's research in 1967 (Ngo 1967), bond link elements or similar kinds of joint elements are often used to represent bond behaviors along discrete reinforcement elements in FEA. On the other hand, tension-stiffening models are often employed to represent the tensile behavior of concrete elements. The tension-stiffening curve is a model derived by drastic simplification of the stress redistribution process through the bond and cracking. It has been implicitly believed that concrete stresses would be double counted if this model is used simultaneously with the discrete reinforcement elements and bond link elements, as **Figs. 1a** and **1b** indicate. **Figures 1c** and **1d** show typical FEA results of simple bending beams. The former is correctly calculated while the latter is over cracked due to doubly counted tension stiffening. Not a few professional engineers and researchers have probably spent considerable time and thought to this problem (e.g. Sato 2003, Ko 2004, Sato 2008, and Kanakubo 2012). However, to

date, no technical literature has discussed the double-counting problem. This study performs example calculations of uniaxial tension specimens (Yamato 2009) in which tension-stiffening models, discrete reinforcement elements, and bond link elements are used simultaneously. The existence or absence of the double-counting effect is discussed based on analyses using smeared crack models and discrete crack models.

## 2. Analyzed specimens

Among the uniaxial tension specimens in one of the authors' study (Yamato 2009), three specimens SD-80SD-D10, SD-100SD-D10, and SD-120SD-D10 are selected for the example calculations. **Table 1** shows the properties of the concrete and steel. The specimen is a rectangular concrete block 1,680 mm in length through which a 10-mm diameter deformed steel bar is embedded. The cross sections of the three specimens are 80 mm × 80 mm, 100 mm × 100 mm, and 120 mm × 120 mm, respectively. The cross sectional area ratios of reinforcement are  $\rho = 1.23\%$ ,  $0.79\%$ , and  $0.55\%$ . Both ends of the reinforcement are unbonded for a length of 40 mm. The remaining bonded length of 1,600 mm is modeled by four-node plane stress concrete elements.

Table 1 Material properties.

Concrete		
Compressive strength	Tensile strength	Elastic modulus
28.6 N/mm <sup>2</sup>	2.44 N/mm <sup>2</sup>	26,800 N/mm <sup>2</sup>
Deformed bar (diameter = 10 mm)		
Yield stress	Tensile strength	Elastic modulus
752 N/mm <sup>2</sup>	931 N/mm <sup>2</sup>	197,000 N/mm <sup>2</sup>

<sup>1</sup>Assistant Professor, Department of Architecture and Architectural Engineering, Kyoto University, Kyoto, Japan.

E-mail: satou@archi.kyoto-u.ac.jp

<sup>2</sup>Associate Professor, Department of Engineering Mechanics and Energy, University of Tsukuba, Tsukuba, Japan.

<sup>3</sup>Professor, School of Management, Kochi University of Technology, Kochi, Japan.

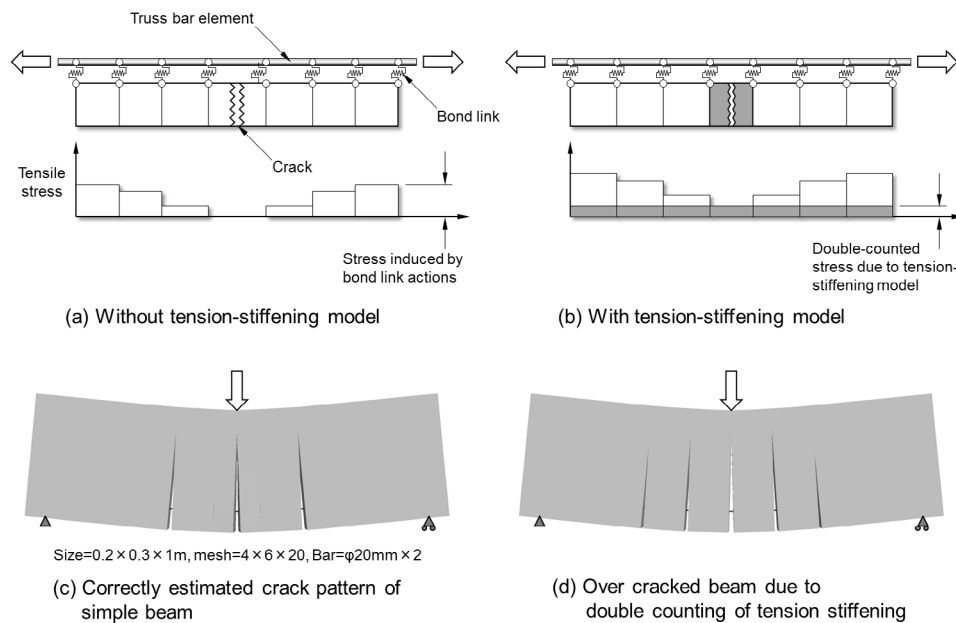


Fig. 1 Double-counting problem caused by simultaneous use of discrete reinforcement elements, bond link elements, and tension-stiffening model.

### 3. Criteria curve of tension-stiffening

To judge the presence or absence of the double-counting effect, a criteria tension-stiffening curve is prepared. This criteria curve is derived from calculations using a difference scheme (Sato 2003). The bond length (half a crack spacing) is discretized into 100 divisions and the distribution of tensile concrete stress is calculated. **Figure 2** shows the assumption of the bond stress-slip relationship adopted in the calculation. When the tensile concrete stress at the midpoint between existing cracks reaches the tensile concrete strength, then a new crack occurs and the crack spacing is halved. The crack spacing is no more halved when the bond stress along the reinforcement cannot induce a tensile concrete stress larger than the tensile strength. The calculation is continued until no more cracks occur and the spacing at this time is defined as the final crack spacing.

**Figure 3a** shows the relationships between the load and elongation of specimens with reinforcement ratios  $\rho = 1.23\%$ ,  $0.79\%$ , and  $0.55\%$ , respectively, while **Fig. 3b** shows the calculation results of the same specimens. The calculation results principally trace the tendency of the tests in that the tension-stiffening effect becomes larger as the cross sectional area of concrete becomes larger, although these tests and calculations must not necessarily match. The calculated crack spacings are 100 mm for specimens with  $\rho = 1.23\%$  and  $0.79\%$  and

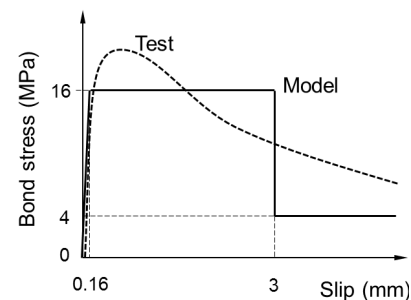


Fig. 2 Assumption of bond stress-slip relationship.

200 mm for  $\rho = 0.55\%$  (**Table 2**). These spacings agree with the test results' tendency that the spacing becomes larger as the reinforcement ratio becomes smaller.

**Figure 4a** shows the calculation result of the tension-stiffening behavior of a specimen with  $\rho = 1.23\%$ . As shown in **Fig. 4**, the up and down of the curve, which are caused by cracking, are smoothed by fitting an averaged multi-linear curve, in an intension to apply it to the concrete elements of the FEA. **Figures 4c** and **4d** show the averaged curves of the specimens of  $\rho = 0.78\%$  and  $0.55\%$ . **Table 3** lists the coordinates of the branches of the multi-linear curve for each specimen. The strains at the second branches of the specimens with  $\rho = 0.79\%$  and  $0.55\%$  are larger than the cracking strain of concrete,  $0.000091$  ( $=2.44 \text{ N/mm}^2 / 268,000 \text{ N/mm}^2$ ), because considerable displacements are in-

Table 2 Calculated final crack spacing.

Reinforcement ratio		$\rho = 1.23\%$	$\rho = 0.79\%$	$\rho = 0.55\%$
Final crack spacing	Test*	73 mm	105 mm	336 mm
	Calculation	100 mm	100 mm	200 mm

\*Crack spacing in test =  $1680 \text{ mm} / (\text{number of transverse cracks} + 1)$

Table 3 Coordinates of branches of multi-linear tension-stiffening curve.

Branch	$\rho = 1.23\%$		$\rho = 0.79\%$		$\rho = 0.55\%$	
	Strain ( $\times 10^{-3}$ )	Stress ratio ( $\sigma_{c1m}/f'_t$ )	Strain ( $\times 10^{-3}$ )	Stress ratio ( $\sigma_{c1m}/f'_t$ )	Strain ( $\times 10^{-3}$ )	Stress ratio ( $\sigma_{c1m}/f'_t$ )
1	0.0	0.0	0.0	0.0	0.0	0.0
2	0.091	1.000	0.112	1.000	0.142	1.000
3	0.175	0.742	0.224	0.719	0.285	0.706
4	0.260	0.628	0.359	0.609	0.481	0.602
5	0.470	0.505	0.689	0.498	0.967	0.493
6	0.838	0.477	1.860	0.438	2.541	0.387
7	1.206	0.440	3.285	0.190	3.437	0.148
8	2.224	0.362	4.149	0.190	6.018	0.042
9	3.720	0.295	6.429	0.037	--	--
10	6.000	0.114	--	--	--	--

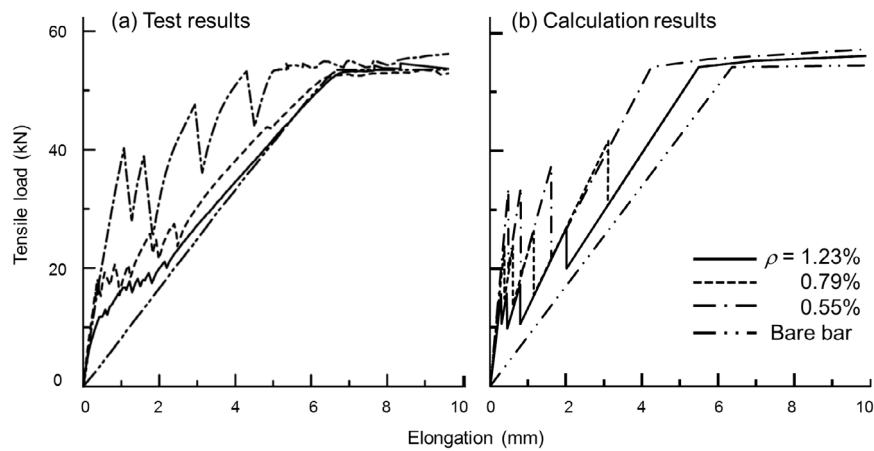


Fig. 3 Relationships between load and elongation (test and analysis).

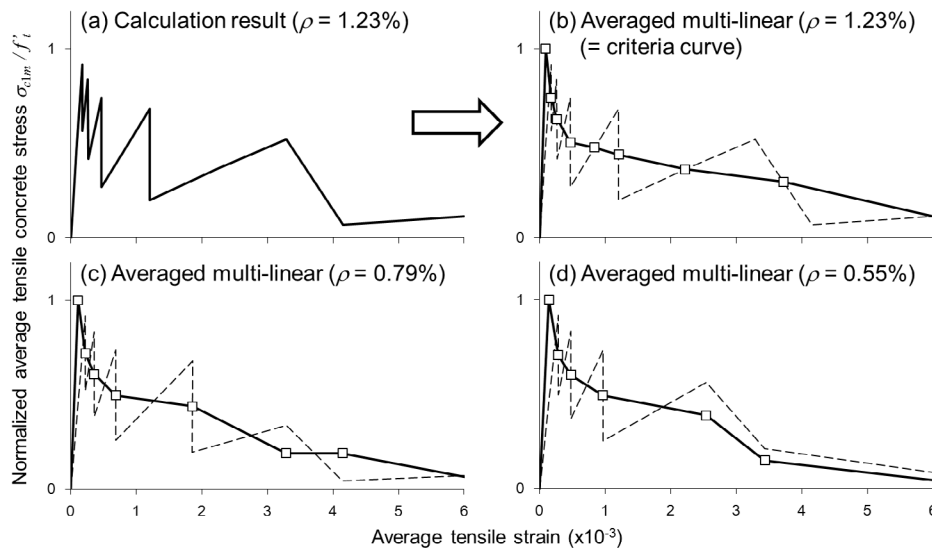


Fig. 4 Averaging of criteria tension-stiffening curve.

duced by bond slips at the cracks.

These multi-linear relationships are employed in the next sections as tension-stiffening models for the concrete elements of FEA and compared as a basic criterion.

#### 4. Finite element modeling: Smeared crack model and discrete crack model

Finite element analyses are conducted by two kinds of modeling (smeared crack model and discrete crack model) and varied element sizes. **Figure 5a** shows mesh

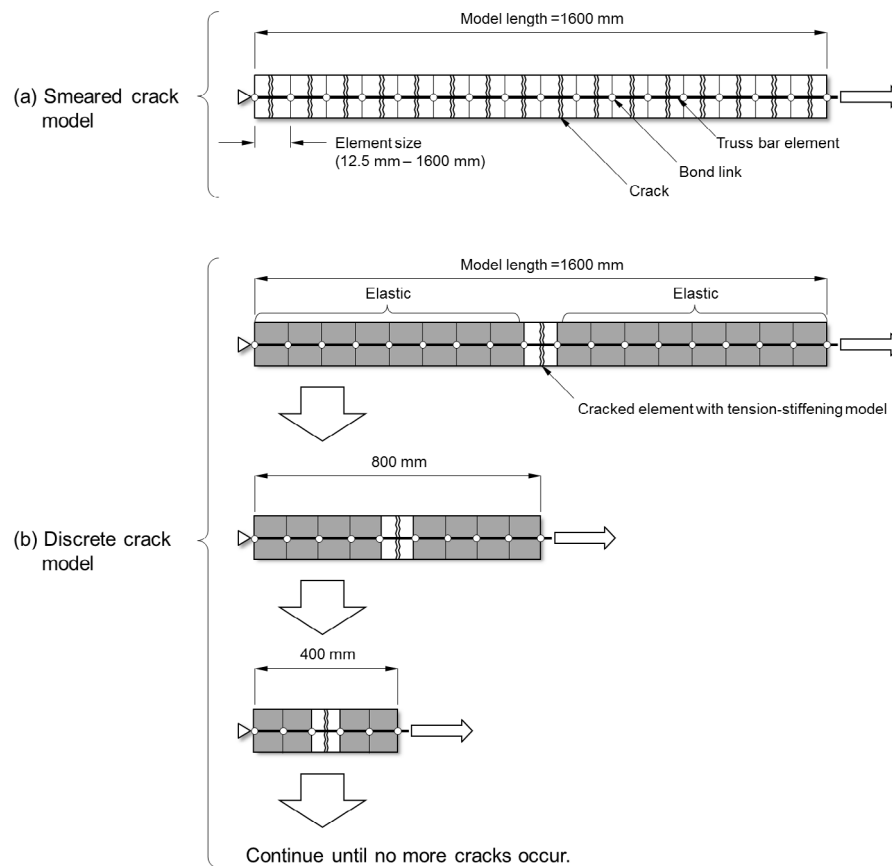


Fig. 5 Mesh divisions (smeared crack model and discrete crack model).

divisions for the smeared crack model while **Fig. 5b** shows that for the discrete crack model. The specimen is divided into two elements along the transverse direction; discrete reinforcement elements and bond link elements are arranged along the longitudinal direction. A prescribed displacement is applied to a node of a reinforcement element at an end of the specimen until the average strain reaches 0.006. The total number of analysis steps is 300. Apparent average tensile concrete stress is calculated as (tensile load – average tensile reinforcement force) / cross sectional area of concrete. The program used is FINAL (Naganuma 2004). The analysis methods of the smeared crack model and discrete crack model are described below.

- (1) Smeared crack model: The tension-stiffening model is applied to all concrete elements. Eight element sizes are used (i.e., 12.5 mm, 25 mm, 50 mm, 100 mm, 200 mm, 400 mm, 800 mm, and 1,600 mm). Therefore, the division along the longitudinal direction is 126 at the maximum and 1 at the minimum.
- (2) Discrete crack model: The discrete crack model generally uses crack link elements, which are inserted in the boundaries between the concrete elements. However, a constant tensile stress may remain in the concrete elements between two cracks if the crack spacing is relatively large along a uniaxial tension specimen, as shown in **Fig. 6**. In finite element analysis, cracks would simultaneously be

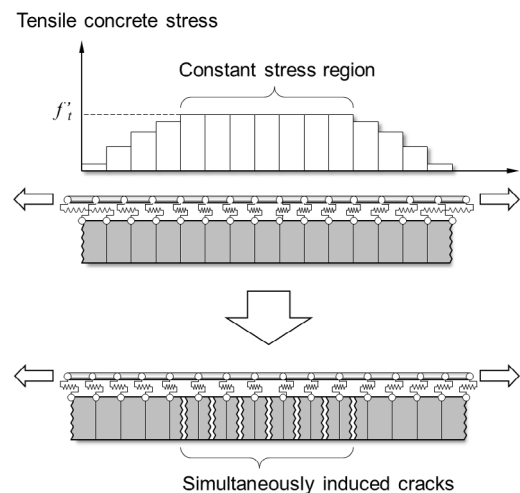


Fig. 6 Simultaneously induced cracks along constant stress region.

induced in all these elements. This problem is solved by the following method. The specimen is divided into an odd number of elements and cracking is allowed only at the center element, to which a tension-stiffening model is applied, as shown in **Fig. 5b**. The rest of the elements are assumed elastic. The calculation begins from a model 1,600 mm long and the length is halved if a crack occurs. This process is repeated until no more cracks occur.

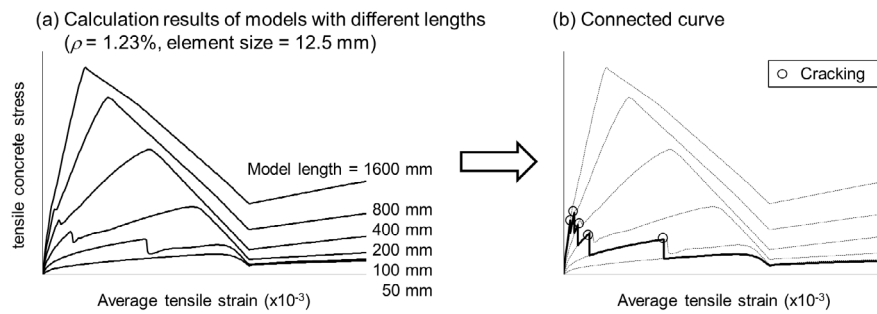


Fig. 7 Connected curve derived from discrete crack analyses.

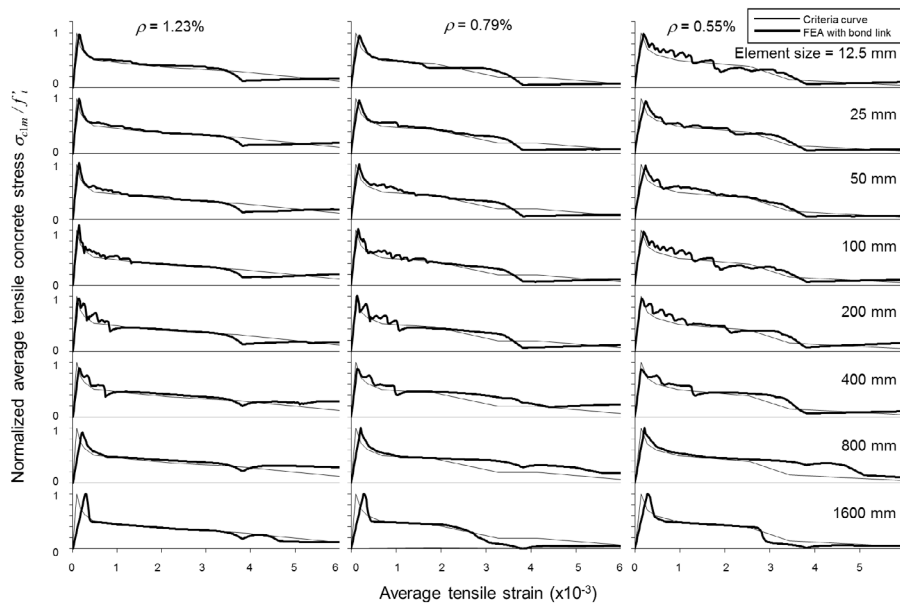


Fig. 8 FEA results of smeared crack models.

**Figure 7a** shows the calculation results of the FE models with different lengths, where the reinforcement ratio  $\rho$  is 1.23% and the element size is 12.5 mm. In this specimen, the cracking process is finished when the model length reaches 25 mm. **Figure 7a** shows the calculation results of six models of with lengths of 1,600 mm, 800 mm, 400 mm, 200 mm, 100 mm, and 50 mm. These six curves are connected at the cracking point of each model so that a single tension-stiffening relationship is prepared, as shown in **Fig. 7b**.

## 5. Smeared crack FE analyses

**Figure 8** shows the results of smeared crack analyses. The figures in the left column show the analysis results of specimens of  $\rho = 1.23\%$ , those in the center column of  $\rho = 0.79\%$ , and in the right column of  $\rho = 0.55\%$ . The first row shows the results for element size 12.5 mm, the second row for 25 mm, and all eight rows show the results for element sizes up to 1,600 mm. The bold lines indicate FE analyses while the fine lines indicate the criteria curves defined in **Fig. 4** and **Table 3**. As shown in **Fig. 8**, the FE analyses largely agree with the criteria curves.

In the smeared crack analyses, cracks occur simultaneously in all elements. Hence, the double-counting effect does not appear because no gradient is induced along the distribution of tensile concrete stress. It must be noted that the bond link elements do not act in smeared crack models. The simultaneous use of discrete reinforcement elements, bond link elements, and a tension-stiffening model is available only when the analysis deals with large slips or pullouts of reinforcements such as bond splitting or pullout of main reinforcements in beam-column joints.

## 6. Discrete crack FE analyses

**Figure 9** shows the results of discrete crack analyses. The figures are arranged in the same manner as **Fig. 8**. As described in the previous section, the model length is repeatedly halved at each occurrence of cracking at the center element. In the case of reinforcement ratio  $\rho = 1.23\%$  and element size 12.5 mm, six models are needed until the final crack spacing becomes 25 mm (**Fig. 7**). The number of models needed varies depending on the reinforcement ratios and element sizes. **Table 4** lists the number of models needed corresponding to each reinforcement ratio and element size. **Figure 9** shows over-

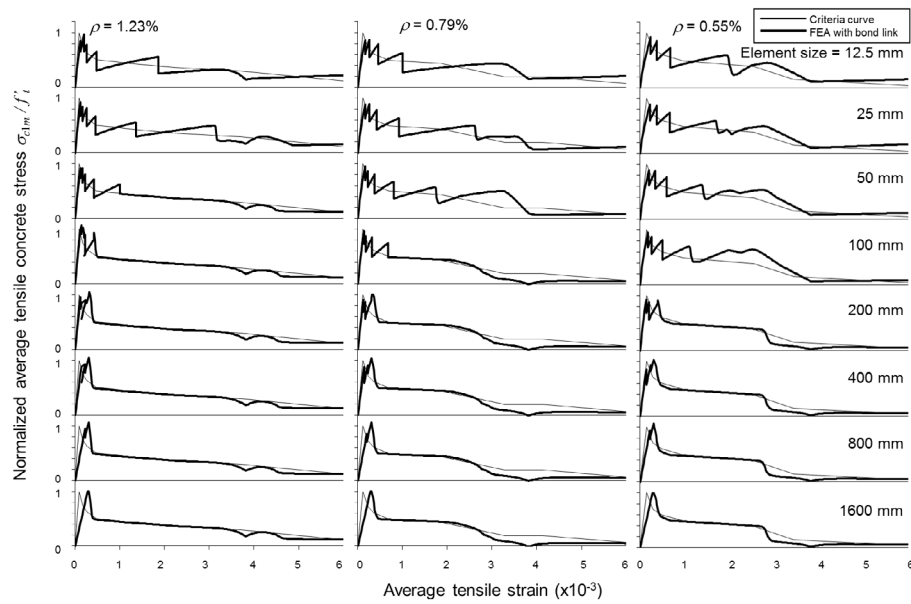


Fig. 9 FEA results of discrete crack models.

all coincidences between the discrete crack analyses and the criteria curves. These results seem as if the double-counting effect does not occur in discrete crack FE analyses.

As described above, however, the final crack spacing becomes 25 mm in the case of  $\rho = 1.23\%$  and element size is 12.5 mm. This spacing is considerably smaller than 100 mm, which is given by the criteria calculation (Table 2). The cause of the underestimation of crack spacing or, in other words, the overestimation of the number of cracks, is that the tensile concrete stress is calculated as a summation of (1) stress due to the tension-stiffening model applied to the center element and (2) stress induced by the slip of bond link elements. The summation overestimates the actual tensile concrete stress and results in over cracking. This is highly related to the double-counting effect, but it appears as a decrease in crack spacing or an increase in the number of cracks rather than as an increase in the tension-stiffening curve.

The asterisks in Table 4 indicate that the final crack spacing is smaller than that given by the criteria calculation shown in Table 2. Crack spacing becomes smaller

than that of the criteria calculation in 13 of the 24 total cases. Crack spacing in the remaining 11 cases is equal or larger than the criteria calculations only because of the element size.

## 7. Discrete crack FE analyses (delayed cracking)

In the previous section, tensile concrete stress is double counted by the tension-stiffening model and the bond link elements and resulted in over cracking. This section attempts analyses in which each cracking is deliberately suspended until a stress due only to the tension-stiffening model becomes equal to the tensile concrete strength  $f'_t$ , as shown in Fig. 10.

Figure 11 shows the analysis results. The final crack spacing becomes equal to the values of the criteria calculations (i.e., 100 mm for  $\rho = 1.23\%$  and  $0.79\%$  and 200 mm for  $\rho = 0.55\%$ ) as shown in Table 5. In contrast, the tension-stiffening curves derived from the analyses considerably overestimate those of the criteria calculations.

Figure 12 shows the coincidence between the FE

Table 4 Number of models needed and final crack spacing in discrete crack FE analyses.

Element size (mm)	$\rho = 1.23\%$		$\rho = 0.79\%$		$\rho = 0.55\%$	
	Crack spacing (mm)	Number of models	Crack spacing (mm)	Number of models	Crack spacing (mm)	Number of models
12.5	25*	6	50*	5	100*	4
25	25*	6	50*	5	100*	4
50	25*	6	50*	5	100*	4
100	50*	5	50*	5	100*	4
200	100	4	100	4	100*	4
400	200	3	200	3	200	3
800	400	2	400	2	400	2
1600	800	1	800	1	800	1

\* Crack spacing smaller than that given by criteria calculation shown in Table 2.

Table 5 Number of models needed and final crack spacing in discrete crack FE analyses (delayed cracking).

Element size (mm)	$\rho = 1.23\%$		$\rho = 0.79\%$		$\rho = 0.55\%$	
	Crack spacing (mm)	Number of models	Crack spacing (mm)	Number of models	Crack spacing (mm)	Number of models
12.5	100	6	100	5	200	4
25	100	6	100	5	200	4
50	100	6	100	5	200	4
100	100	5	100	5	200	4
200	100	4	100	4	200	4
400	200	3	200	3	200	3
800	400	2	400	2	400	2
1600	800	1	800	1	800	1

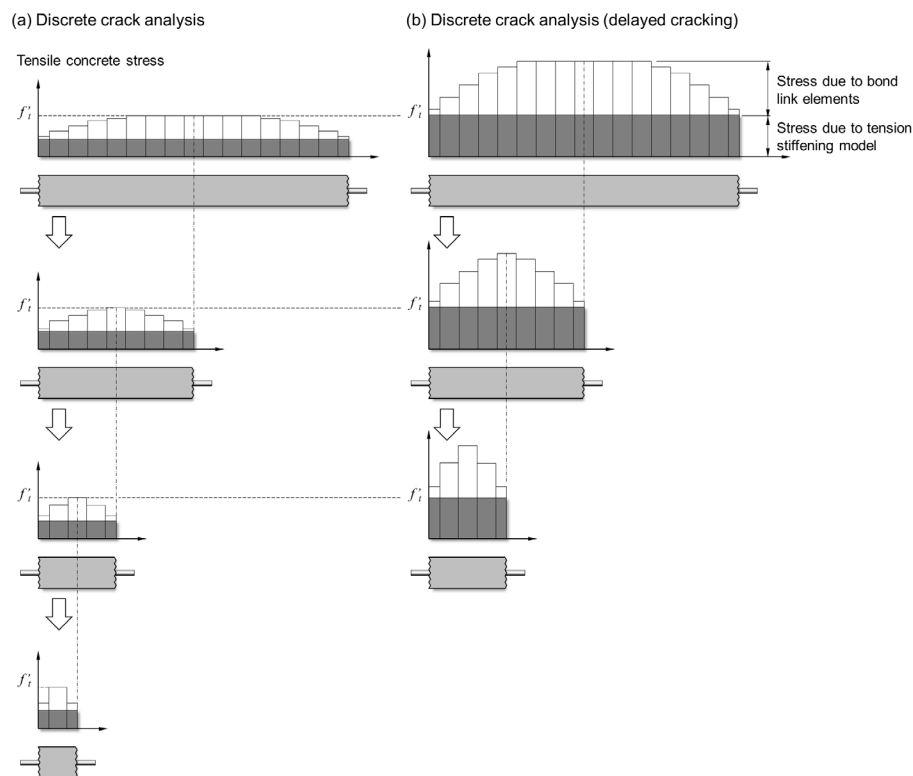


Fig. 10 Comparison of distributions of tensile concrete stresses in discrete crack analyses.

analyses and the criteria curves. The vertical axis represents the ratio of the area enveloped by the curve of FE analysis to that of the area enveloped by the criteria curve while the horizontal axis represents the element size in logarithmic scale. The enveloped area ratios of the smeared crack models are almost constant at 1.0 regardless of the reinforcement ratios and element sizes as **Fig. 12a** shows. The ratio becomes greater than 1.0 at element sizes of 800 mm and 1,600 mm, but these overestimations are caused because excessively large element sizes deteriorate the accuracy of analyses. Similarly, **Fig. 12b** shows the constant envelope area ratios of 1.0 regardless of reinforcement ratios and element sizes for the discrete crack models. On the other hand, the ratios of the delayed cracking calculations of the discrete crack models shown in **Fig. 12c** indicate that the analyses overestimate tension-stiffening by 148% to 196% if the element size is smaller than the

final crack spacing. The results show the typical effect of double counting.

## 8. Conclusions

The double-counting problem associated with the simultaneous use of discrete reinforcement elements, bond link elements, and tension-stiffening models is discussed with example analyses of uniaxial tension specimens. The analyses employ three different models of the finite element method: (1) smeared crack analyses, (2) discrete crack analyses, and (3) discrete crack analyses with delayed cracking. The analyses are performed by varying the reinforcement ratios and element sizes. The following observations can be made based on this study.

- (1) Smeared crack analyses with tension-stiffening models cause no double-counting effect although



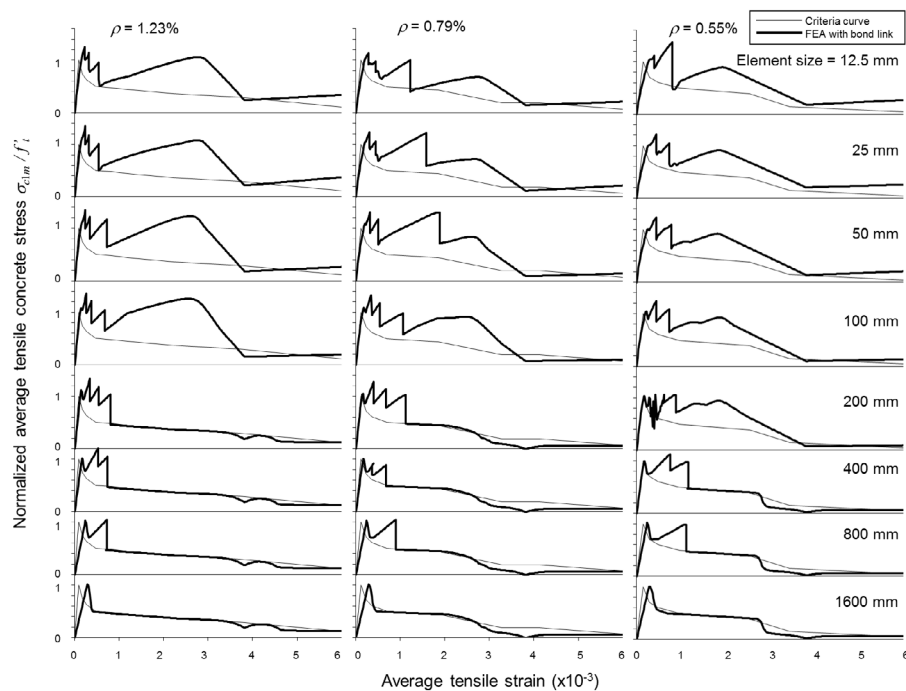


Fig. 11 FEA results of discrete crack models (delayed cracking).

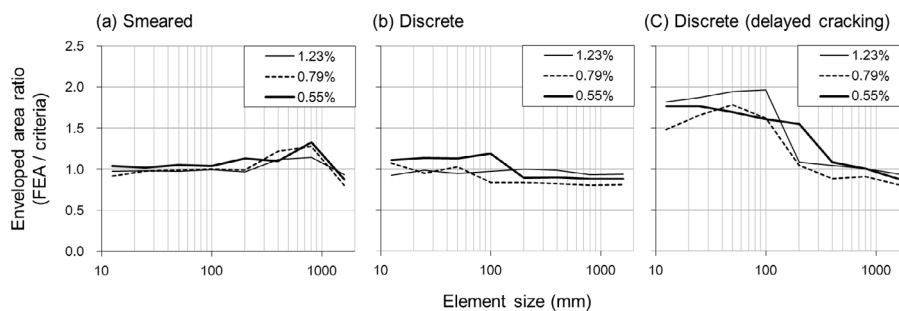


Fig. 12 Enveloped area ratio of tension-stiffening curves (FEA/criteria curve).

no slip is induced in the bond link elements so that the link elements do not contribute to stress redistributions. The simultaneous use of discrete reinforcement elements, bond link elements, and a tension-stiffening model is available only when the analysis deals with large slips or pullouts of reinforcements such as bond splitting or pullout of main reinforcements in beam-column joints.

- (2) The double-counting effect appears in discrete crack analyses when the element sizes are equal or smaller than the final crack spacing. However, in these analyses, the double-counting effect does not result in overestimations of tension-stiffening relationships but does result in underestimations of final crack spacing due to overcracking.
- (3) Discrete crack analyses with delayed cracking cause the typical double-counting effect where the tension-stiffening relationships are overestimated. The overestimation ratios of the enveloped area of the analyzed tension-stiffening curve to those given by the criteria calculations range from 148% to 196%.

This study was conducted as one of the activities of the Japan Concrete Institute Technical Committee on Bond Behavior and Constitutive Laws in RC (JCI-TC092A).

## References

- Kanakubo, T., Sato, Y., Uchida, Y., Watanabe, K. and Shima, H., (2012). "Japan Concrete Institute TC activities on bond behavior and constitutive laws in RC (Part 3 Application of Constitutive Laws for FEA)." *Proceedings of Bond in Concrete 2012*, Brescia, Italy, 1, 105-112.
- Ko, H. and Sato, Y., (2004). "Analysis of FRP-strengthened RC members with varied sheet bond stress-slip models." *Journal of Advanced Concrete Technology*, 2(3), 317-326.
- Naganuma, K., Yonezawa, K., Kurimoto, O. and Eto, H., (2004). "Simulation of nonlinear dynamic response of reinforced concrete scaled model using three-dimensional finite element method." *Proceedings of 13th World Conference on Earthquake Eng. (WCEE 13)*, Vancouver, BC, Canada, 586.

- Ngo, D. and Scordelis, A. C., (1967). "Finite element analysis of reinforced concrete beams." *Journal of ACI*, 64(3), 152-163.
- Sato, Y. and Vecchio, F. J., (2003). "Tension stiffening and crack formation in reinforced concrete members with fiber-reinforced polymer sheets." *ASCE Journal of Structural Engineering*, 129(6), 717-724.
- Sato, Y. and Ko, H., (2008). "Modeling of reinforcement buckling in RC columns confined with FRP." *Journal of Advanced Concrete Technology*, 6(1), 195-204.
- Yamato, N. and Kanakubo, T., (2009). "Prediction method of crack width in reinforced concrete members Part 1: Theoretical solution by the bi-linear model of bond constitutive law." *Journal of Structural and Construction Engineering, Architectural Institute of Japan*, 74(640), 1137-1143.